Engineering with Computers (2026) 42:211
https://doi.org/10.1007/s00366-026-02428-9

ORIGINAL ARTICLE

FLOWS: a model to simulate water and solutes fluxes in agricultural and environmental systems. 1. Theory and applications with intercode benchmarking

Antonio Coppola[1] · Angelo Basile[2] · Alessandro Comegna[3] · Caterina Fenu[4] · Anna Concas[4] · Fabio Pili[4] · Shawkat B. M. Hassan[1]

Received: 13 March 2026 / Accepted: 9 September 2026
© The Author(s) 2026

Abstract
FLOWS (FLOws of Water and Solutes in soils) is a dynamic physically-based model to simulate water flow and solute transport in the soil–plant–atmosphere system. The numerical code was written in MATLAB. One-dimensional vertical transient water flow is simulated by numerically solving the 1D form of the Richards equation (RE) using an implicit, backward, finite differences scheme with explicit linearization. As for the solutes, the code solves the 1D Advection Dispersion equation (ADE) by an explicit, central difference scheme, allowing for a relatively easy inclusion of non-linear adsorption and other non-linear processes. The model produces information on the time evolution of (among many other outputs): soil water contents and pressure potentials in the soil profile; solute (tracers, adsorbed, volatile and reactive solutes) concentrations in the soil profile; water and solute uptake and actual evapotranspiration for simulated crops; deep percolation water and solute fluxes; root uptake of water and solutes, also in presence of water and osmotic stresses; water fluxes and related solute fluxes to runoff; drainage water fluxes and related solute fluxes; irrigation fluxes computed by the model; and temperature in the soil profile. Compared to other existing models, some specificities of FLOWS model are: (1) integrated simulation of carbon, nitrogen and phosphorus transformations and transport contextually to the simulation of water contents and fluxes; (2) macroscopic root uptake; (3) irrigation management, by allowing to optimize the time scheduling and volumes according to some criterion based on the average pressure head in the root zone; (4) the possibility of running multi-site simulations, which may be especially important for spatially distributed simulations; and (5) an interactive graphical user interface, allowing the user to easily handle even large input files and seeing the simulation results by graphical display of the main output variables.

Keywords Physically-based dynamic agrohydrological modelling · Richards equation · Advection-dispersion equation · Web-based GUI

1 Introduction

The movement of water in the soil and associated solute transport have a role of primary importance in many applications in the field of hydrology and agriculture. In the sound management of irrigation water, in relation to specific environmental conditions and cropping systems, knowledge of local water flow conditions in zones explored by the root systems is indispensable. Once the irrigation method has been established, only knowledge of the laws governing water flow allows the necessary irrigation frequencies and rates to be established to optimise the distribution of soil moisture, reducing within established limits the effects of

✉ Shawkat B. M. Hassan
shawkat.hassan@unibas.it

[1] Department of Chemical and Geological Sciences, University of Cagliari, 09124 Cagliari, Italy

[2] Institute for Mediterranean Agricultural and Forestry Systems, National Research Council, 80055 Portici, NA, Italy

[3] Department of Agricultural, Forestry, Food and Environmental Sciences, University of Basilicata, 85100 Potenza, Italy

[4] Department of Mathematics and Computer Science, University of Cagliari, 09124 Cagliari, Italy

Published online: 26 October 2026

water stress and containing water wastage. Only by studying water dynamics in soil can the contribution of groundwater to water consumption be quantitatively determined. Moreover, the water volumes infiltrating into the soil due to rainfall are strictly linked and governed by the laws of water flow in the soil. No evaluation of water quantities being added to groundwater circulation can be made without first determining the water volumes moving in the zone between the soil surface and the aquifer.

Knowledge of water fluxes, velocities and contents is also indispensable to study the flow of solutes and pollutants and to predict all exchanges, whether chemical or microbiological, occurring in the soil. Within environmental protection initiatives, great weight is attributed to the continuous contribution of solutes characterising any agricultural activity, especially if intensive. Nor should one underestimate the hazards of non-agricultural solute fluxes, and the need to dispose of wastewater, muds and industrial effluent.

To evaluate the nature of the risk represented by the presence of these solutes, it is important to define the processes governing their movement downward from the soil surface through the vadose zone as far as the aquifer. Only if we know such transport processes can optimal management plans be developed for environmental control with a view to preventing degradation phenomena.

The complexity of such flow processes has encouraged the widespread use in the sector of soil hydrology of increasingly sophisticated mathematical models of varying levels of dimensionality corresponding as closely as possible to real phenomena, which can supply quantitative evaluations also in the presence of highly complex systems, such as soil–plant–atmosphere continuum (SPAC).

In general, such models are based on laws governing water flow and all the physical and chemical processes affecting water transport. These laws have been widely confirmed by experiments and are often reported also in papers in disciplines collateral to soil hydrology [1, 2]. Water flow is studied with reference to a porous medium which, on a macroscopic scale, may be considered continuous and in which the various quantities and physical properties are considered functions of position and time. Reference is generally made to isothermal flow processes, to a Newtonian liquid phase and interconnected gaseous phase with a pressure equal to that of the atmosphere.

Several complex, physically-based models simulating water flow and solute transport in unsaturated–saturated soil are now available (see, for example, LEACHM—[3]; SWAP—[4]; RZWQM—[5]; HYDRUS—[6]). These models can simulate a broad range of flow and transport processes and, with appropriate boundary and initial conditions, may be employed to deal with many agricultural and environmental problems.

However, in many cases, these models require the users to have specific and deep skills about soil and solute hydrology, limiting in many cases their use for practical applications by agricultural and environmental managers. Actually, nowadays models are increasingly requested to answer to specific and practical management issues by farmers, by providing responses in terms of the irrigation water, organic matter, nutrients, to be supplied to a specific crop under specific soil and environmental scenarios. In this direction, there are many models more specifically oriented to agricultural systems, such as DAISY [7], EPIC [8], APSIM [9], DSSAT [10], which can be used as practical water and nutrients management tools under different agro-environmental scenarios.

In all the cases, these models may become much more widespread once they have been provided with user-friendly graphics-based interfaces allowing their use even by users not fully involved in the modelling topic.

In this context, the model FLOWS [11] described in this paper tries to integrate positive aspects of different models and to make modelling as much user-friendly as possible. It systematizes work already presented in several previous papers [12–18] by incorporating the simulation codes into a client–server architecture, which allows users to interact directly with the model through a web browser.

The model simulates water flow by solving the RE and the solute transport (tracers, adsorbed, volatile and reactive solutes) by solving the ADE and thus allows approaching general environmental problems related to water and contaminant transport by a fully physically based approach. For agricultural management purposes, FLOWS allows the integrated simulation of organic and inorganic carbon, nitrogen and phosphorus chemical transformations and transport contextually to the simulation of water contents and fluxes. It also allows irrigation management, by optimizing the irrigation time and volumes according to a criterion based on the average pressure head in the root zone. FLOWS also simulates water and nutrient fluxes to artificial drainage, as well as to runoff.

The user is driven in all these model applications by a graphical model interface where all the input data and parameters may be set. The interface guides the user in all the settings by providing suggestions and warnings, making settings faults unlikely. This way, the model allows for running simulations even users not perfectly within the field of physically based hydrological models.

All the input (node and time conditions, profile settings, vegetation settings, solute settings) may be provided as excel tables which have simply to be uploaded from the main interface.

For agricultural applications, the user is provided with a flexible table allowing to input several organic and inorganic

fertilizers and a table where to input irrigation management settings.

All the outputs are also provided as excel files, each including a matrix with the evolution of the output variable given for all the simulation depth nodes and time steps. Additionally, at the end of each simulation run, the model produces plots of the water content, pressure heads, water fluxes and solute concentrations for selected times and depths, allowing a rapid evaluation of the results and goodness of the simulation run.

Additionally, the model offers the possibility of running multi-site simulations, which may be especially important for spatially distributed simulations, as well as for simulations carried out under stochastic framework (Montecarlo, for example). A detailed description of the model may be found in the model handbook [11].

In this paper (paper 1), we will schematically summarise the development of the various components of FLOWS. Applications of the model with different top and bottom boundary conditions will also be shown, along with an intercode benchmarking with the well-known HYDRUS 1D software. Appendix is dedicated to describing the nonlinear solution procedure and time-step-control algorithm and added an explicit description of the approach used to evaluate water and solute mass conservation.

In a companion paper (paper 2—FLOWS: A model to simulate water and solutes fluxes in agricultural and environmental systems. 2. Modules for specific applications in agro-hydrological modeling), more details will be given on the specialized components related to agricultural management, such as irrigation computed by the model, organic matter decomposition, organic and inorganic nutrient transformations and transport, fluxes of water and solutes to artificial drainage and runoff, along with selected applications of these components related to real irrigation, nutrient and drainage datasets.

2 General description of the model

FLOWS is a dynamic physically based model, written in MATLAB, simulating water flow and solute transport in the soil–plant–atmosphere system by numerically solving the 1D form of the Richards equation (RE) for water flow and the 1D Advection Dispersion equation (ADE) for solute transport. Heat flow is also simulated in the model since several parameters related to nutrients reactions and transport and various partitioning and production coefficients are strongly temperature dependent.

Figure 1 provides a schematic view of all the processes involved in the current version of FLOWS. The main processes (the red blocks in the figure) form the basis for the description of all the other related processes in the blue blocks.

FLOWS simulates all the processes shown in Fig. 1 in an integrated modelling approach, so that they are simulated together in the same simulation time step, Δt. The lower part of the figure also summarises the main outputs of the model. Obviously, the code may be easily modified to produce specific outputs, based on the above list, requested for specific agro-environmental applications (i.e., water storage in a given depth interval, travel time of a solute at selected depths, etc.).

2.1 Soil water flow

FLOWS simulates 1D vertical transient water flow by numerically solving the Richards equation (Eq. 1) using an implicit, backward, finite differences scheme with explicit linearization [4]:

$$C(h)\frac{\partial h}{\partial t} = \frac{\partial}{\partial z}\left(K(h)\frac{\partial h}{\partial z} + K(h)\right) - S_w \quad (1)$$

where C(h) = dθ/dh [L^{-1}] is the soil water capacity, h [L] is the soil water pressure head, t [T] is time, z [L] is the vertical coordinate being positive upward, K(h) [$L\ T^{-1}$] the hydraulic conductivity and S_w [T^{-1}] is a sink term describing water uptake by plant roots, S_r, and/or lateral water drainage, S_{dr}, so that $S_w = S_r + S_{dr}$.

1D soil column assumption is acceptable in applications where vertical gradients are dominant, such as evapotranspiration, infiltration, rootzone storage, groundwater recharge and leaching [19, 20]. Lateral fluxes, like artificial drainage, groundwater lateral fluxes and root uptake, can be represented by dedicated sink terms [21]. Spatial variability can be represented by the multisite simulations (Sect. 4).

2.1.1 Hydraulic properties

Richards' equation requires the water retention function, θ(h), and the hydraulic conductivity, K(h) or K(Se), function to be known. These functions interrelate pressure head, h, water content, θ, and hydraulic conductivity, K. Several water retention (WRC) and hydraulic conductivity (HCC) functions can be selected in the model (see Table 1).

2.1.1.1 Water retention curves (WRC) All the curves are expressed in terms of effective saturation $S_e = (q - q_r)/(q_s - q_r)$, where q_s and q_r are the saturated and residual water contents, respectively. S_e is to be considered as a cumulative

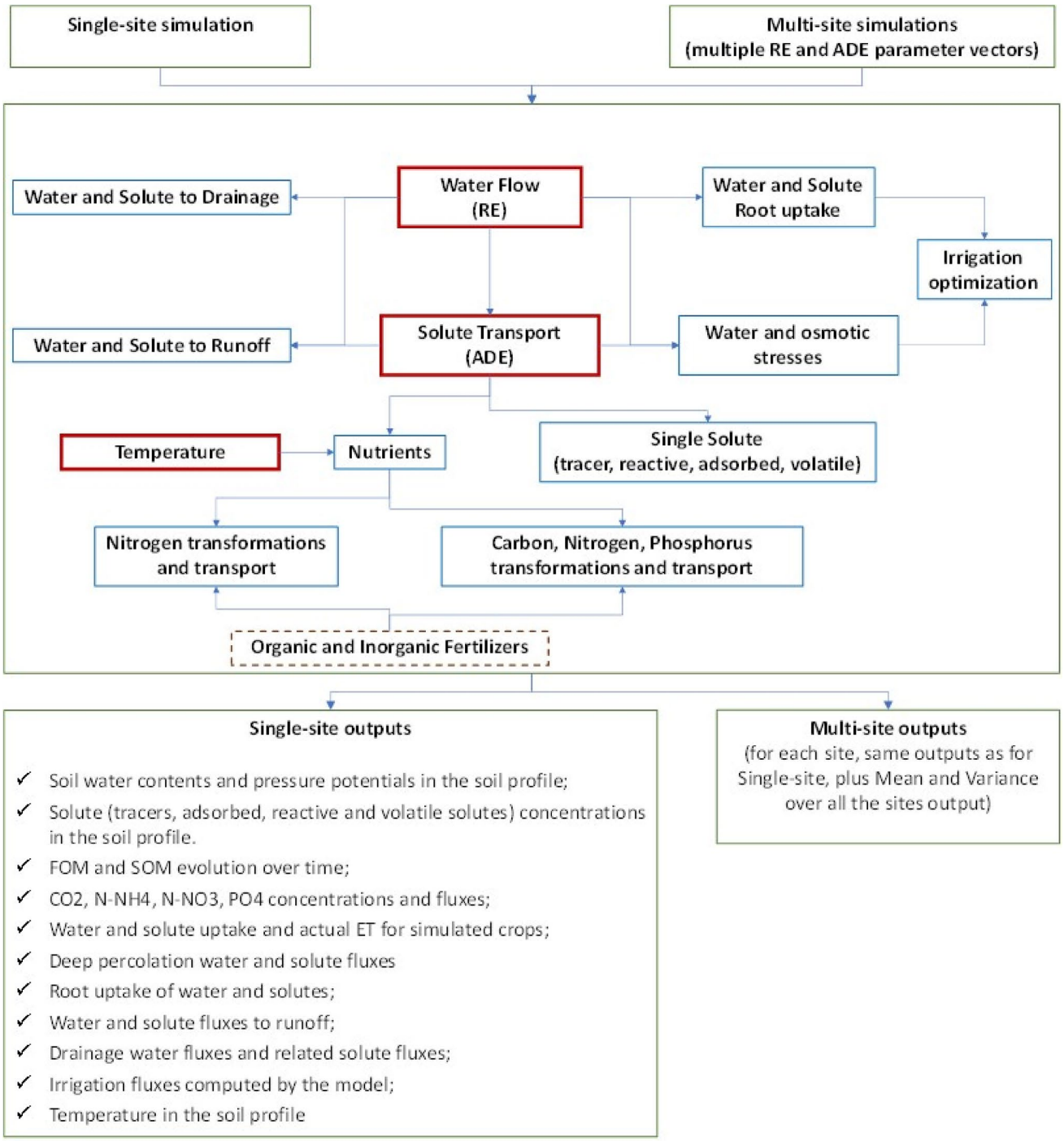


Fig. 1 Schematic view of all the processes simulated in FLOWS, their interactions and simulation options. The model provides all the outputs listed in the lower box. In the case of multiple simulations (for example spatially distributed simulations or repeated simulations in stochastic frameworks), all the outputs are provided for each of the input parameter vectors, along with the average and variance of each output

distribution function of pore size with a density function $f(h)$, which may be expressed by:

$$f(h) = \frac{dSe}{dh} \tag{2}$$

In the case of unimodal pore size distribution, FLOWS allows opting for either the WRC model proposed by van Genuchten [22] (Eq. 5) or that proposed by Russo [23] (Eq. 11). Both the models are reported in Table 1. In the van Genuchten model, α_{vg} and n are shape parameters. In the

Table 1 The WRC and HCC models included in FLOWS

van Genucthen–Mualem	WRC	$S_e = \frac{\theta-\theta_r}{\theta_s-\theta_r} = \left[1+\lvert\alpha_{VG}h\rvert^n\right]^{-m}$	(5)
	HCC	$K_r(S_e) = \frac{K(S_e)}{K_0} = S_e^{\tau}\left[1-\left(1-S_e^{1/m}\right)^m\right]^2$	(6)
		$m = 1-1/n$	
Durner–Mualem	WRC	$S_e = \varphi_1(1+\alpha_{RS}h)\exp(-\alpha_1 h) + \varphi_2\left[\frac{1}{1+(\alpha_{VG}h)^{n_2}}\right]^{m_2}$	(7)
	HCC	$K_r(S_e) = \frac{K(S_e)}{K_0} = \left(\sum_{i=1}^{2}\varphi_i S_{e,i}\right)^{\tau}\left\{\frac{\sum_{i=1}^{2}\varphi_i\alpha_{VG,i}\left[1-\left(1-S_{e,i}^{1/m_i}\right)^{m_i}\right]}{\sum_{i=1}^{2}\varphi_i\alpha_{VG,i}}\right\}^2$	(8)
Ross & Smettem	WRC	$S_e = \varphi_1(1+\alpha_{RS}h)\exp(-\alpha_1 h) + \varphi_2\left[\frac{1}{1+(\alpha_{VG}h)^{n_2}}\right]^{m_2}$	(9)
	HCC	$K_r(h) = \frac{K(h)}{K_0} = S_e^{\tau}\left[\sum_{i=1}^{2}\varphi_i\eta_i(h)/\sum_{i=1}^{2}\varphi_i\eta_i(0)\right]^2$	(10)
		$\eta_1(h) = \alpha_{RS}\exp(\alpha_{RS}h)$	
		$\eta_2(h) = \alpha_{VG}n_2B\left(S_e^{1/m_2}, m_2+1/n_2, 1-1/n_2\right)$	
Russo–Gardner	WRC	$S_e = \frac{\theta-\theta_r}{\theta_s-\theta_r} = [\exp(-0.5\alpha_{GR}h)(1+0.5\alpha_{GR}h)]^{\left(\frac{2}{\mu_R+2}\right)}$	(11)
	HCC	$K_r(h) = \frac{K(h)}{K_0} = exp(-\alpha_{GR}h)$	(12)

Russo model, α_{GR} the parameter appearing in the Gardner's model for hydraulic conductivity (see next section on HCC models) and is related to the pore size distribution, while μ_R is a parameter related to tortuosity.

In natural soils, the presence of aggregates frequently results in a retention function curve having at least two points of inflection. To represent such behaviour, a double porosity approach can be used, which assumes that the pore space from θ_r to θ_s consists of two $f_i(h)$ distributions obtained by Eq. 2, each occupying a fraction ϕ_i of that pore space [24]. FLOWS allows using two different double porosity models, respectively proposed by Durner [25] (Eq. 7) and Ross and Smettem [26] (Eq. 9) (see again the Table 1). Both the models describe the WRC of the whole porous medium by linearly combining two sub-curves, one for structural pores and the other for textural pores. The Durner model uses a van Genuchten type curve for each pore domain, where $\alpha_{VG,i}$, n_i and m_i still represent the shape parameters for each of the partial curves, whereas the Ross and Smettem model assumes a single parameter curve for the structural domain, described by the shape parameter α_{RS}, The parameter ϕ_i is used as a weighting factor of the total pore space fraction to be attributed to each of the two subcurves.

2.1.1.2 Hydraulic conductivity curves (HCC) FLOWS allows opting for two different HCC approaches.

The first is the approach proposed by Mualem [27], which is based on the capillary bundle theory and relates relative hydraulic conductivity, K_r, to $f(h)$ by the equation:

$$K_r(h) = \frac{K(h)}{K_0} = S_e^{\tau}[\eta(h)/\eta(0)]^2$$
$$\eta(h) = \int_{-\infty}^{\infty} h^{-1} f(h)\, dh \tag{3}$$

in which K_0 is the hydraulic conductivity at $h = 0$, and τ is a parameter accounting for the dependence of the tortuosity and the correlation factors on the water content.

For the bimodal case, Eq. 8 becomes:

$$K_r(h) = \frac{K(h)}{K_0} = S_e^{\tau}\left[\sum_{i=1}^{2}\varphi_i\eta_i(h)/\sum_{i=1}^{2}\varphi_i\eta_i(0)\right]^2 \tag{4}$$

with parameters as defined earlier.

In FLOWS, the WRC models proposed by van Genuchten [22], Durner [25] and Ross and Smettem [26], all are coupled to the Mualem model for deriving analytical equations for the HCC based on the *f(h)* functions (see Table 1).

The van Genuchten HCC analytical equation (Eq. 6) has been obtained by imposing $m = 1 - 1/n$. The Durner–Priesack HCC (Eq. 8) comes from an analytical solution of the Eq. 4, with $\eta_i(h) = \alpha_{VG,1}n_iB\left(S_e^{1/m_i}, m_i+1/n_i, 1-1/n_i\right)$. Similarly, the Ross and Smettem HCC (Eq. 10) comes from the solution of Eq. 4 with $\eta_1(h) = \alpha_{RS}\exp(\alpha_{RS}h)$.

The second approach is that proposed by Gardner [28]. The Gardner HCC (Eq. 12) is generally coupled to the Russo model for WRC (Eq. 11), with the parameter α_{GR} being a sorptive number related to the pore size distribution of the medium, with larger values associated with coarse-textured

soils. It is also the reciprocal of capillary length parameter, λ_c, ($\alpha_{GR} = \lambda_c^{-1}$), which can be interpreted as the length of the capillary fringe or the air-entry pressure head value.

2.1.2 The sink term, S_w

FLOWS calculates a sink term, S_w, by summing up water uptake by plant roots, S_r, and lateral water drainage, S_{dr}, so that $S_w = S_r + S_{dr}$.

2.1.2.1 Root water uptake sink term, S_r FLOWS calculates the root water sink term, S_r, in Eq. 1 according to a macroscopic approach, frequently adopted in hydrologically oriented soil–plant–atmosphere continuum modelling for describing plant water uptake [29, 30].

Specifically, the potential root water uptake flux per unit depth at a specific depth, $S_{r,p}$ [T^{-1}], is simulated by distributing potential transpiration, T_p [$L\ T^{-1}$], over the root zone depth, D_r [L], on the basis of a normalized root density distribution, $g(z)$ [L^{-1}], with depth z.

The function $g(z)$ distributes the potential transpiration rate, T_p, through the root zone in proportion to the root distribution [29, 30]:

$$S_{r,p}(z) = g(z)\,T_p \tag{13}$$

with

$$\int_0^{Dr} g(z)\,dz = 1 \tag{14}$$

and thus

$$T_p = \int_0^{Dr} S_{r,p}(z)\,dz \tag{15}$$

Several root density distributions, $g(z)$, may be selected in the model for simulating the sink term in Eq. 1, assuming root distributions to be either homogeneous [30] or variable with depth [31–33], the latter accounting for the fact that in a moist soil the roots can mainly extract water from the upper root zone layers. Table 2 summarises the four schemes of root density distribution implemented in FLOWS.

Table 2 The four normalized root-density distributions implemented in FLOWS

Uniform [30]	$g(z) = \frac{1}{D_r}$	(16)
Triangular [32]	$g(z) = \frac{2(D_r - z)}{D_r^2}$	(17)
Vrugt et al. [33]	$g(z) = \frac{\omega(z)}{\int_0^{D_r} \omega(z)dz}$ $\omega(z) = \left(1 - \frac{z}{D_r}\right) exp\left(\frac{p_z}{D_r}\lvert z^* - z\rvert\right)$	(18)
Logistic	$g(z) = \frac{b\,exp\left[b\left(c - \frac{z}{D_r}\right)\right]}{D_r\left\{1 + a\,exp\left[b\left(c - \frac{z}{D_r}\right)\right]\right\}^{\frac{1}{a}+1}}$	(19)

The Uniform distribution over the whole root zone only requires the maximum root depth, D_r [L]. The Prasad-type triangular distribution [32], assumes the root water uptake at the bottom of the root zone, D_r, equal to zero. The Vrugt distribution is based on the following dimensionless spatial root distribution, $\omega(z)$:

$$\omega(z) = \left(1 - \frac{z}{D_r}\right) exp\left(\frac{p_z}{D_r}\lvert z^* - z\rvert\right) \tag{20}$$

where p_z [–] and z^* [L] are empirical parameters. The model allows for non-symmetrical root water uptake. The non-symmetry with soil depth is determined by the ratio of the p_z value for $z \le z^*$ and the p_z value for $z > z^*$. To reduce the number of parameters to be optimized, p_z may be set to unity for $z > z^*$, whereas it is fitted for $z \le z^*$.

The Logistic distribution is based on shape coefficients a, b and c and the maximum depth D_r of the roots.

2.1.2.2 Water and osmotic stress functions Low water contents and/or the presence of soluble salts in the soil lower the total hydraulic head and may reduce the water fluxes to the roots, thus reducing root activity and water uptake. Reduction coefficients to decrease the maximum water uptake according to the water and osmotic stresses may be calculated independently and multiplied to calculate the actual root uptake, T_a, as:

$$S_r = \alpha_w(h)\,\alpha_s(h_{os})\,S_p = \alpha_w(h)\,\alpha_s(h_{os})\,g(z)\,T_p \tag{21}$$

with α_w and α_s being reduction factors depending on the local (at a given z) water pressure head, h [L] and osmotic head, h_{os} [L], respectively.

Accordingly,

$$T_a = \int_0^{Dr} S_r(z)\,dz \tag{22}$$

and

$$\frac{T_a}{T_p} = \int_0^{D_r} g(z)\,\alpha_w(h)\,\alpha_s(h_o)\,dz = \beta(h, h_{os}) \tag{23}$$

with T_a being the actual transpiration rate and β a dimensionless water stress index integrated over the whole rooted profile [34, 35], providing a measure of total plant stress. A value of β equal to 1 indicates that there is no stress in

the soil root zone and that the actual transpiration rate T_a is equal to the potential transpiration rate T_p.

FLOWS allows calculating water, α_w, and solute stress, α_s, either independently or combined, according to the approaches summarized in Table 3.

2.1.2.3 Water stress reduction factor, α_w Feddes and Raats [29] reviewed various functional forms for α_w that have been proposed over the years. Two models are implemented in FLOWS for water stress:

- A piecewise linear reduction function proposed by Feddes [30] (Eq. 24 in Table 3), parameterized by four critical values of the water pressure head, $h_4 < h_3 < h_2 < h_1$. In this model, water uptake is reduced at high- and low-pressure heads. Uptake is at the potential rate when $h_3 \leq h \leq h_2$, drops off linearly when $h > h_2$ or $h < h_3$, and becomes zero when $h \leq h_4$ (permanent wilting pressure head range) or $h \geq h_1$ (anaerobiosis pressure head range). As the value of h_3 is expected to be a function of evaporative demand, either a low or high evaporative demand h_3 value may be set, identified respectively as h_{3low} and a h_{3high};
- A smooth, S-shaped reduction function proposed by van Genuchten [36] (Eq. 25) with adjustable parameters p_1 and h_{50}, the latter being the water pressure head where uptake is halved.

2.1.2.4 Salinity stress reduction factor, α_s FLOWS includes several functional forms, which are frequently adopted to describe uptake reduction due to salinity (see amongst others [29, 38]). The salinity uptake reduction function can be written in terms of concentration, electrical conductivity of either the soil water or the soil saturation extract, or osmotic pressure head [37, 40–42]. FLOWS uses the osmotic pressure head, h_{os}, form. Two models are implemented in FLOWS:

- A piecewise linear (threshold–slope) function proposed by Mass and Hoffman [37] (Eq. 26), with adjustable parameters a and b, often referred to as the salinity threshold and slope, respectively;
- a S-shaped salinity-stress function proposed by van Genuchten and Hoffman [38], in terms of pressure head, similar to that for the water stress reduction factor, where p_2 and $h_{os,50}$ are the adjustable parameters, the latter being the osmotic pressure head where uptake is halved.

The osmotic potential, expressed as osmotic head h_{os}, is assumed to be a linear function of soil solution salinity, σ_w (dSm^{-1}), according to U. S. Salinity Laboratory Staff [43]:

$$h_{os} = -360\sigma_w \tag{30}$$

where 360 is a factor to convert the salinity-based values (dSm^{-1}) to osmotic head (cm).

2.1.2.5 Combined water and salinity stress FLOWS includes additive and/or multiplicative combined stresses [44]. A generalized model for additive stresses (Eq. 28 in Table 3) is obtained by assuming that water uptake occurs in response to some weighted sum of the soil water pres-

Table 3 Models for water and osmotic stress reduction factors implemented in FLOWS

Feddes water stress [30]	$\alpha_w(h) = \begin{cases} \frac{h-h_4}{h_3-h_4}, & h_3 > h > h_4 \\ 1, & h_2 \geq h \geq h_3 \\ \frac{h-h_1}{h_2-h_1}, & h_1 > h > h_2 \\ 0, & h \leq h_4 \text{ or } h \geq h_1 \end{cases}$	(24)
van Genuchten water stress [36]	$\alpha_w(h) = \frac{1}{1+\left(\frac{h}{h_{50}}\right)^{p_1}}$	(25)
Mass and Hoffman osmotic stress [37]	$\alpha_s(h_{os}) = \begin{cases} 1, & a \leq h_{os} \leq 0 \\ 1 + b(h_{os} - a), & a > h_{os} > a - \frac{1}{b} \\ 0, & h_{os} \leq a - \frac{1}{b} \end{cases}$	(26)
van Genuchten and Hoffmann osmotic stress [38]	$\alpha_s(h_{os}) = \frac{1}{1+\left(\frac{h_{os}}{h_{os,50}}\right)^{p_2}}$	(27)
Combined water and osmotic stress by Skaggs et al. [39]	$\alpha(h, h_{os}) = \frac{1}{1+\left[\frac{\alpha_1 h + \alpha_2 h_{os}}{h_{os,50}}\right]^{p_2}}$	(28)
	Additive	
	$\alpha(h, h_{os}) = \frac{1}{1+\left(\frac{h}{h_{50}}\right)^{p_1}} \frac{1}{1+\left(\frac{h_{os}}{h_{os,50}}\right)^{p_2}}$	(29)
	Multiplicative	

sure and osmotic heads. A simple additivity results when $\alpha_1 = \alpha_2 = 1$. Although additivity has been inferred from a number of laboratory and field experiments, e.g., [45–49], its general applicability remains uncertain [50], especially for field conditions subject to relatively wide ranges in pressure heads (wetting/ drying cycles).

Linear or weighted additivity is only one of several possibilities for combining the effects of water and salinity stress. Another approach presumes that water and salinity effects are multiplicative. In the general case this leads to:

$$\alpha(h, h_{os}) = \alpha(h)\alpha(h_{os}) \tag{31}$$

which, in the case of S-shaped curves, gives the Eq. 29.

2.1.2.6 Drainage sink term, S_{dr} FLOWS includes the artificial drainage in the Richards equation as a sink term based on the Hooghoudt's theory for lateral flow to the drains (Fig. 2). It has been demonstrated that a 1-D solution to the flow and transport system, combined with Hooghoudt theory, gives similar results as a 2-D solution with explicit representation of drain tiles based on the previous studies, provided that an appropriate implementation of the Hooghoudt theory is used. This issue has been analysed in details by Mollerup et al. [51].

Water flows toward the drain anytime the water table is located above either a drainpipe or a on open field drain. According to Hooghoudt [52], the steady state drain flux per unit surface area q_{dr} can be computed as:

$$q_{dr} = \frac{8K_b D_{eq} D_a + 4K_a D_a^2}{L_{dr}^2} \tag{32}$$

where K_a is the hydraulic conductivity of the saturated layer above the drain level and K_b is the hydraulic conductivity of the layer below the drain level. L_{dr} is the distance between the drains. The water table height above the drain at $0.5L_{dr}$ is denoted as D_a (corresponding to h in the Hooghoudt's work). D_{eq} is the equivalent drain depth depending on the vertical distance between the drains and the impervious layer, D_{imp}, as well as on the drain hydraulic radius, R_{dr}.

Details on the solution of Eq. 32 used in FLOWS will be given in the paper 2 devoted to FLOWS modules for specific applications in agro-hydrological modelling.

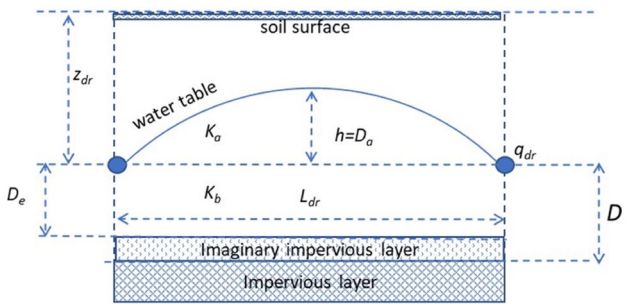


Fig. 2 Schematic view of the system and parameters involved in the Hooghoudt's equation

2.1.3 Runoff calculation

The model calculates the runoff water fluxes if the top-boundary fluxes, q_{surf}, exceed the soil surface infiltration capacity (Hortonian mechanism) or when the profile is completely saturated (Dunnain mechanism). The former is calculated using the maximum infiltration velocity at soil surface, fs_{max}:

$$fs_{max} = K_{m,max}\left(\frac{h_1 - h_{surf,max}}{\Delta z_{top}} - 1\right) \tag{33}$$

where $K_{m,max}$ is the average between the soil surface and the first node's soil hydraulic conductivities, h_1 is the soil water pressure head in the top node and $h_{surf,max}$ is the maximum pressure head allowed at the soil surface, which is set by the user.

When $q_{\text{surf}} > fs_{max}$, the code switches the upper boundary from a flux to a head condition, setting the top boundary pressure head equal to $h_{surf,max}$. If the additional condition $|q_{\text{surf}}| > K_0$ is satisfied at the top node, the excess water flux $(q_{\text{surf}} - fs_{max})$ becomes runoff.

Regarding the Dunnian runoff mechanism, at each time step Δt, the model calculates the water storage at full saturation and the actual water storage over the entire simulation domain. When the difference between these two quantities falls below a predefined tolerance, the entire incoming surface flux, q_{surf}, during the current time step is converted to runoff.

3 Solute transport in soils

FLOWS solves the advection–dispersion equation (ADE) for prediction of solute transport (agrochemicals, salts, heavy metals, …):

$$\frac{\partial \theta C}{\partial t} + \rho_b \frac{\partial C_s}{\partial t} + \frac{\partial \theta_g C_g}{\partial t} = -\frac{\partial qC}{\partial z} + \frac{\partial}{\partial z}\left(\theta D_h \frac{\partial C}{\partial z}\right) + \frac{\partial}{\partial z}\left(\theta_g D_g^s K_H \frac{\partial C}{\partial z}\right) - S_s \tag{34}$$

including linear and non-linear adsorption, linear volatilization, linear decay and proportional root uptake in unsaturated/saturated soil. In the equation, C [M L^{-3}], C_s [M M^{-1}] and C_g [M L^{-3}], are the solute concentrations in the liquid, adsorbed and gaseous phases, respectively, q [L T^{-1}] is the

darcian water flux, ρ_b [M L^{-3}] is the bulk density, D_h [L^2 T^{-1}] the hydrodynamic dispersion coefficient, D_g^s is the dispersion coefficient in the gaseous phases [L^2 T^{-1}], θ_g is the volumetric air content in soil, S_s [ML^{-3} T^{-1}] is a source-sink term for solutes, K_H is the dimensionless Henry constant. Hydrodynamic dispersion is related to the molecular diffusion constant of the substance in bulk water, D_0 [L^2 T^{-1}], and the average pore water velocity, $v = q/\theta$, as:

$$D_h = \lambda v + \eta(\theta) D_0 \tag{35}$$

where λ [L] is the dispersivity and η a tortuosity coefficient.

By introducing an effective dispersion coefficient, D_e,

$$D_e = D_h + \frac{\theta_g D_g^s K_H}{\theta} \tag{36}$$

the Eq. 34 becomes

$$\frac{\partial \theta C}{\partial t} + \rho_b \frac{\partial C_s}{\partial t} + \frac{\partial \theta_g C_g}{\partial t} = -\frac{\partial qC}{\partial z} + \frac{\partial}{\partial z}\left(\theta D_e \frac{\partial C}{\partial z}\right) - S_s. \tag{37}$$

3.1 Linear and non-linear solute sorption

FLOWS assumes equilibrium interaction between the solution, C, and adsorbed, C_s, concentrations of solute on soil particles. The adsorption isotherm relating C_s and C is described in the code by either a *linear* or the *Freundlich* non-linear equation. The *Freundlich* isotherm is a flexible function for many organic and inorganic solutes:

$$C_s = K_F C^p \tag{38}$$

where p (dimensionless) is the Freundlich exponent, commonly less than unity for most adsorbing solutes and enhanced with decreasing C, and K_F [L^3M^{-1}] is the Freundlich partitioning coefficient [53]. The *linear* isotherm is a special case where the Freundlich exponent is unity and $K_F = K_D$ (the slope of the linear isotherm) is known as the distribution coefficient.

3.2 Linear solute volatilization

The gaseous phase is also considered in FLOWS to account for volatilization and gas phase diffusion of organic contaminants. Actually, even if the latter may decay mostly because of chemical and microbiological degradation, volatilization may be equally important for some substances such as pesticides. A linear equilibrium volatilization is assumed, so that gaseous, C_g, and liquid, C, concentrations are linearly related through the dimensionless Henry constant, K_H:

$$C_g = K_H C. \tag{39}$$

3.3 Solute source-sink term

The solute source-sink term in Eqs. 34 and 37 comes from the contribution of solute decay, $S_{s,\mu}$, solute root uptake, $S_{s,r}$ and solute losses coming from drainage fluxes, $S_{s,dr}$:

$$\begin{aligned} S_{s,\mu} &= \mu(\theta C + \rho_b C_s) \\ S_{s,r} &= K_r S_r C \\ S_{s,dr} &= S_{dr} C \\ S_s &= S_{s,\mu} + S_{s,r} + S_{s,dr} \end{aligned} \tag{40}$$

where μ is a first order decay rate coefficient of transformation (T^{-1}), accounting for linear decomposition, and K_r [–] is a factor for solute root uptake, accounting for positive or negative selection of solute ions relative to the amount of root water uptake S_w.

3.4 Solute transfer from soil solution to runoff water

In FLOWS, solute flux, q_s, across the soil surface interface is related to the difference in concentration between soil solution, C, and runoff water, C_{run}, through a mass transfer coefficient, k_{run}:

$$q_s(0,t) = -\theta D_h \frac{\partial C}{\partial z} + v\theta C\Big|_{z=0} = (-\theta k_{run}[C(0,t) - C_{run}]) \tag{41}$$

The equation above accounts for the convective and dispersive modes of transfer between soil and runoff water [54]. Convective mass transport is directed downward, while diffusive-dispersive transport is directed upward. k_{run} is mainly controlled by the diffusion coefficient but it is also influenced by flow characteristics such as runoff water depth, rainfall intensity and duration, surface roughness.

Assuming that C_{run} can be neglected, the equation above becomes:

$$-D_h \frac{\partial C}{\partial z} + (v + k_{run}) C\Big|_{z=0} = 0 \tag{42}$$

applying for finite values of k_{run}, from which the flux to runoff may be calculated.

3.5 Calculation of the Osmotic Potential for salinity stress

For the calculation of the salinity stress reduction factor, α_s, FLOWS requires the osmotic potential, h_{os}, to be used in the Mass and Hoffman approach [37] and in the van Genuchten

and Hoffman approach [38], as well as in the combined approach. The code uses the concentration coming from the ADE solution for the calculation of the h_{os} values in all the nodes.

Firstly, the code calculates the soil solution electrical conductivity, EC as

$$EC = C * \frac{10^6}{640} \tag{43}$$

with EC in dSm^{-1} and C in gcm^{-3}.

Thus, the osmotic potential, h_{os}, is obtained as:

$$h_{os} = 3.6EC. \tag{44}$$

4 Multisite simulations

FLOWS allows for simulations in multiple profiles (multi-site simulations). For each simulation profile, the model produces a set of outputs and store them in a specific folder. At the end of the multiple simulations, the model calculates two additional folders, respectively with the average and with the variance of the values of each output variable. The model also produces an output with a list of the failed simulations (with the corresponding failure flag related to convergence problems). The multi-site configuration may be especially useful in the following cases:

1. Simulations to be carried out on several soil profiles in a large area characterized by a spatial variability of the soil hydraulic properties. This may be required, for example, to calculate distributed outputs, such as (among many others): irrigation needs at district scale; deep percolation fluxes of water and solutes to analyse groundwater recharge and/or groundwater vulnerability; etc.
2. Uncertainty Analyses and/or Sensitivity Analysis requiring simulation to be carried several times with different soil hydraulic parameters coming from probability density functions for each of them; and
3. Simulations to be carried out with spatially variable vegetation properties, e.g., K_c, LAI and D_r.

5 The FLOWS graphical interface for direct inputs

FLOWS operates within a MATLAB environment and is accessible through a dedicated web interface: https://flows.unica.it/. For user accessibility, a **client–server architecture** has been implemented. This allows users to interact with the model directly from their browser, without requiring local installations or configurations. The server executes the MATLAB routines and handles all the computational load, while the client interface provides a simple and intuitive access point. The server is equipped with a processor AMD Ryzen Threadripper PRO 7975WX (Advanced Micro Devices, Inc.) with 32 cores/64 threads and 8-channel DDR5 ECC memory. For demanding scientific simulations and parallel workloads, it can provide several times the performance of a typical desktop PC, especially when the software efficiently uses many CPU cores.

Upon accessing the FLOWS website, users can authenticate with their personal login credentials. Once logged in, two options are available:

- **Start a new FLOWS project**, initializing a fresh simulation setup.
- **Load an existing project**, retrieving previously saved configurations and results (see Fig. 3).

The architecture is designed to separate clearly the **user interaction layer** (web front-end built on Vue.js) from the **computational engine** (MATLAB running on the server). Communication between the two layers is managed through dedicated APIs that ensure reliable data transfer, project persistence, and monitoring of the simulation status.

Projects and results will be stored on the server in a future release, allowing users to resume work at any time and from any device. At the current stage, this functionality is still under development. Simulation progress and outputs (soil water content, pressure heads, solute concentrations, evapotranspiration, etc.) are displayed in real time via the interface, while detailed result files remain available for download.

This architecture guarantees:

- **Accessibility**: no need for local MATLAB licenses or configuration.
- **Scalability**: server-side resources can be adapted to handle multiple simultaneous users.
- **Reproducibility**: all project data remain stored and versioned on the server.
- **Security**: access is restricted to authorized users through individual login credentials.

5.1 FLOWS simulation configuration options

FLOWS allows to build a simulation configuration tailored to specific boundary and initial conditions, as well as to the intended simulation objectives (Fig. 4).

Through the *Simulation* menu, FLOWS enables the selection of either a *point-based* configuration, suitable for analysing flow and transport processes at the local scale

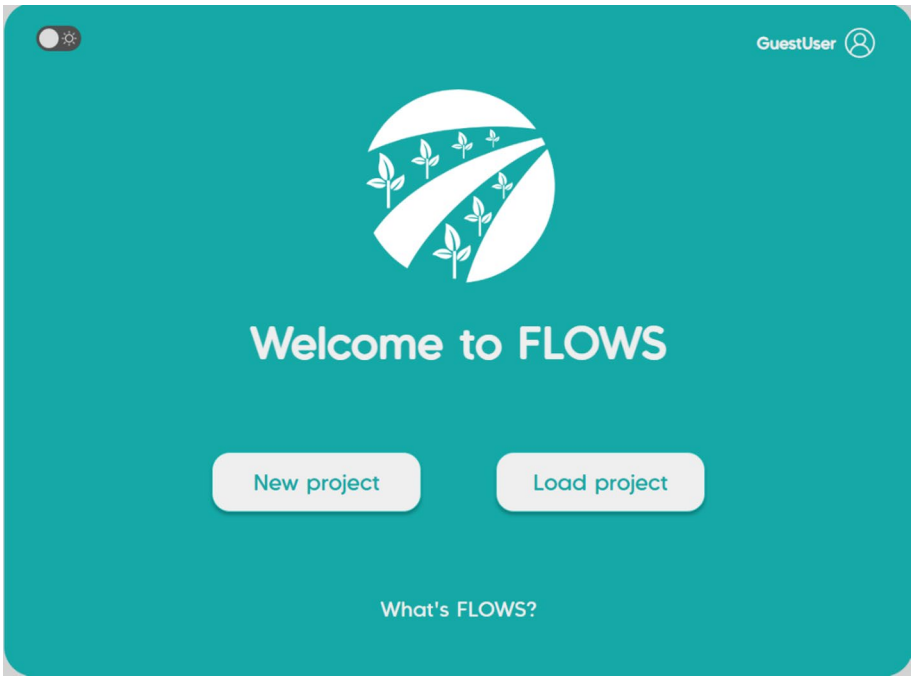


Fig. 3 Web window to start FLOWS

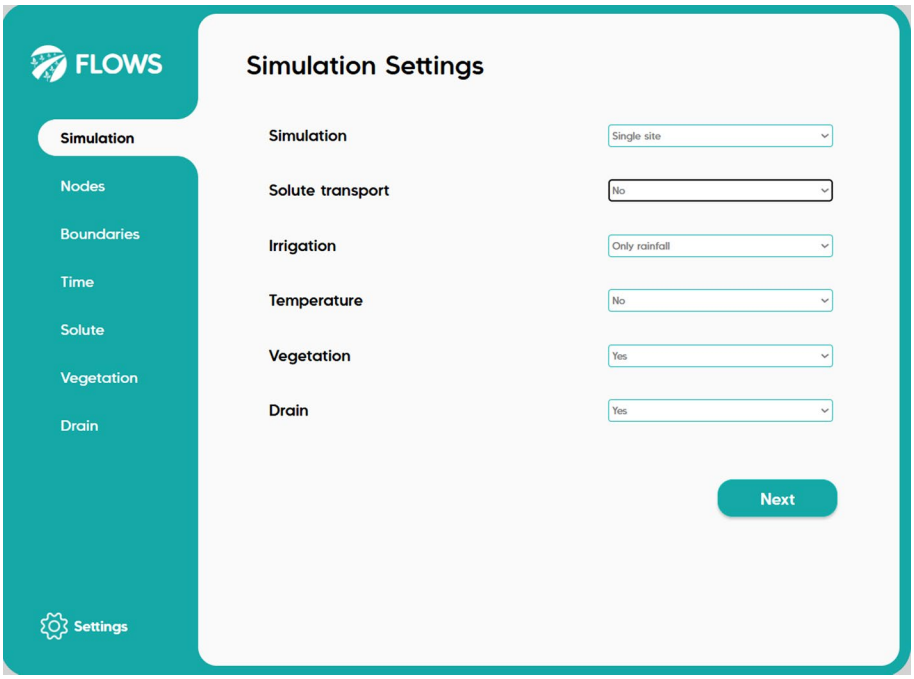


Fig. 4 Simulation settings block

(e.g., localized contamination), or a *multisite* configuration, which allows simultaneous simulations across multiple sites. The latter option is particularly relevant for applications such as irrigation planning and management at the sector or irrigation-district scale, as well as for assessing groundwater vulnerability to diffuse pollution (e.g., from agricultural sources).

Within the *Simulation* menu, FLOWS allows selecting different solute transport configurations, such as: (1) no solute transport, (2) Solute transport simulated by the Advection–Dispersion equation, which may be suitable when transport of a single solute (a tracer, a pesticide,…) has to be simulated; (3) Nitrogen transformation and transport simulations by solving the Advection–Dispersion equation twice, once for N-NH_4 and once for N-NO_3, with appropriate exchange and source-sink terms; (4) Carbon, nitrogen and phosphorus transformation and transport, according to the transformation-transport chain which will be described in detail in the companion paper.

By the *Irrigation* menu, FLOWS allows simulation of different irrigation scenarios: (1) no irrigation, where rainfall is the only water input; (2) Model-driven irrigation, in which FLOWS determines irrigation timing and volumes according to predefined criteria described in Sect. 2.1 in the companion paper; (3) User-defined irrigation volumes, where the model accounts for irrigation amounts actually applied by the farmer; (4) Irrigation based on daily evapotranspiration requirements, calculated as potential evapotranspiration multiplied by irrigation efficiency factors.

Through the *Temperature* menu, the model allows for simulating the temperature evolution along the soil profile according to the combined approach provided by Wijk and De Vries [55], based on the superposition of the annual and daily sinusoidal fluctuation around a constant value of the soil.

The *Vegetation* menu allows users to include or exclude vegetation form simulations. When vegetation is included, plant growth is represented in a static approach, with vegetation growth provided as model inputs in terms of Leaf Area Index (LAI), reference evapotranspiration (ET_r), crop coefficients (K_c), and maximum rooting depth (D_r). Since LAI, ET_r, K_c and D_r are time-variable inputs, they are given by the user in the "Time" settings menu as daily inputs for the simulated period. Additional parameters include critical pressure head and osmotic head thresholds, used to compute water and salinity stress effects on root water uptake, as well as root distribution profiles.

Bare soil conditions represent a special case of this option, in which *LAI* and *Dr* are set to zero over time, and *Kc* is set to the bare-soil value to convert ETr into potential soil evaporation (Ep).

When vegetation is excluded, the upper boundary condition must be imposed directly, either as a prescribed flux or pressure head. This option is typically used for simulating laboratory experiments conducted under controlled boundary conditions.

Finally, the *Drain* menu allows users to account for the presence or absence of artificial drainage systems. When drainage is included, water fluxes to drains are simulated using the Hooghoudt approach. Solute fluxes to drainage are calculated by multiplying the simulated drainage water fluxes by solute concentrations at the model nodes where drainage is active.

For further details on the use of FLOWS web-based interface, see Coppola et al. (2025).

5.2 Model output

At the end of the simulation FLOWS will produce an output folder including output files excel (xlsx) format. The Table 4 provides a list of the output files, with a description of the variables recorded in the output files.

6 Benchmarking (intercode comparison)

The reliability of FLOWS in numerical simulations has been evaluated by comparing the model results to those coming from HYDRUS 1D simulation for a set of water flow and

Table 4 Output of FLOWS

Output file content (as a function of time and depth)	Instantaneous output	Time-Cumulative output
Pressure heads (L)	**X**	
Water contents (L^3L^{-3})	**X**	
Water capacity (the derivative of the water retention curve) ($L^3L^{-3}L^{-1}$)	**X**	
Water fluxes (LT^{-1})	**X**	**X**
Sink (water uptake) (T^{-1})	**X**	**X**
Artificial Drainage losses (T^{-1})	**X**	**X**
Solute concentrations (ML^{-3})	**X**	
Solute mass ($ML^{-2}\ T^{-1}$) leaving the soil profile by artificial drainage	**X**	**X**
Ammonium nitrogen (N-NH4) solute concentrations (ML^{-3})	**X**	
Nitrate nitrogen (N-NH4) solute concentrations (ML^{-3})	**X**	
Phosphorus (P-PO4) solute concentrations (ML^{-3})	**X**	
CO2 mass ($ML^{-2}\ T^{-1}$) produced in the soil profile by root and microbial respiration	**X**	
Ammonium nitrogen (N-NH4) mass ($ML^{-2}\ T^{-1}$) leaving the soil profile by artificial drainage	**X**	**X**
Nitrate nitrogen (N-NO3) mass ($ML^{-2}\ T^{-1}$) leaving the soil profile by artificial drainage	**X**	**X**
Phosphorus (P-PO4) mass ($ML^{-2}\ T^{-1}$) leaving the soil profile by artificial drainage	**X**	**X**
Water fluxes (LT^{-1}) at top and bottom boundary as a function of time	**X**	**X**
Water and solute fluxes to runoff (LT^{-1}) as a function of time	**X**	**X**
Irrigation fluxes (LT^{-1}) (gross and net irrigation) in the case of irrigation computed by the model	**X**	**X**

solute transport processes involving different top and bottom boundary conditions.

This intercode comparison is especially effective as both the models are based on the same fundamental equations to describe water flow (Richard's equation) and solute transport (Advection–Dispersion equation). Both the codes use similar strategies to adapt time stepping to a convergence criterium, allowing the time step size to increase when the code converges rapidly and decrease when there are convergence problems. Both the codes allow to set the several top and bottom boundary conditions, both constant or variable over time: potential and fluxes at the upper boundary, potential, fluxes and hydraulic gradient at the bottom boundary. Initial conditions may be given as pressure heads, which can be either constant along the soil profile or variable node by node. They also allow to use both unimodal and bimodal hydraulic properties as input for different soil layers. Also, when evaporation and precipitation occur simultaneously, both the models subtract evaporation from precipitation and applies net precipitation to the soil.

In the following, a comparison between FLOWS and HYDRUS 1D results will be illustrated for a simulation carried out under real, quite complex, soil-groundwater-climatic conditions.

Table 5 summarizes the top and bottom boundary conditions and soil and vegetation parameters used for the intercode benchmarking simulations (both for FLOWS and HYDRUS 1D). The top boundary conditions for water flow simulations were set as time-variable fluxes [cm/d] representing both precipitation and irrigation. The bottom boundary conditions were set as time-variable pressure heads [cm]. The initial conditions were set as a constant pressure head of −100 cm in all the simulation nodes. As for the solute transport simulations, a top boundary condition was set as a pulse with a concentration of 0.04 g/cm^3 and a duration of one day. The top and bottom boundary conditions were set as zero concentrations, meaning that the pulse was the only source of solute.

Figure 5 provides a graphical view of the time-variable top and bottom boundary conditions, as well as of the time-variable vegetation conditions used for the simulation.

Figure 6 presents a comparison of key variables simulated by the two models under identical conditions (see Table 5). Specifically, the figures illustrate evapotranspiration fluxes, as well as water fluxes, pressure heads, and solute concentrations at a depth of 20 cm, as predicted by the FLOWS model (solid orange lines) and the HYDRUS model (blue open circles). For clarity and improved visibility, the third graph from the top is the fluxes of the second graph but only within the range between −0.2 and 0 cm/d.

The graphs in Fig. 7 were obtained under the same scenario as before but assuming free drainage (unit hydraulic

Table 5 Water and solute top and bottom boundary conditions and soil and vegetation parameters used for the intercode benchmarking simulations

Soil								
Number of layers in the soil profile						4		
Hydraulic properties model						van Genuchten–Mualem		
Layer depths and hydraulic parameters								
Layer	Depth from the soil surface (cm)	Bulk density (g/cm^3)	θ_s	θ_r	α_{VG}	n_{VG}	K_0 (cm/d)	τ
1	40	1.67	0.361	0.017	0.033	1.187	118.08	0.5
2	60	1.74	0.316	0.047	0.033	1.187	429.37	0.5
3	100	1.78	0.309	0.047	0.033	1.187	479.96	0.5
4	140	1.83	0.298	0.049	0.033	1.187	360.84	0.5
Vegetation								
Root distribution		Uniform						
Water Uptake reduction function		Feddes						
Feddes parameters for water uptake reduction		hI	hII		hIIIH	hIIIL		hIV
		− 1	− 10		− 400	− 600		− 8000
Extinction factor for LAI		0.5						

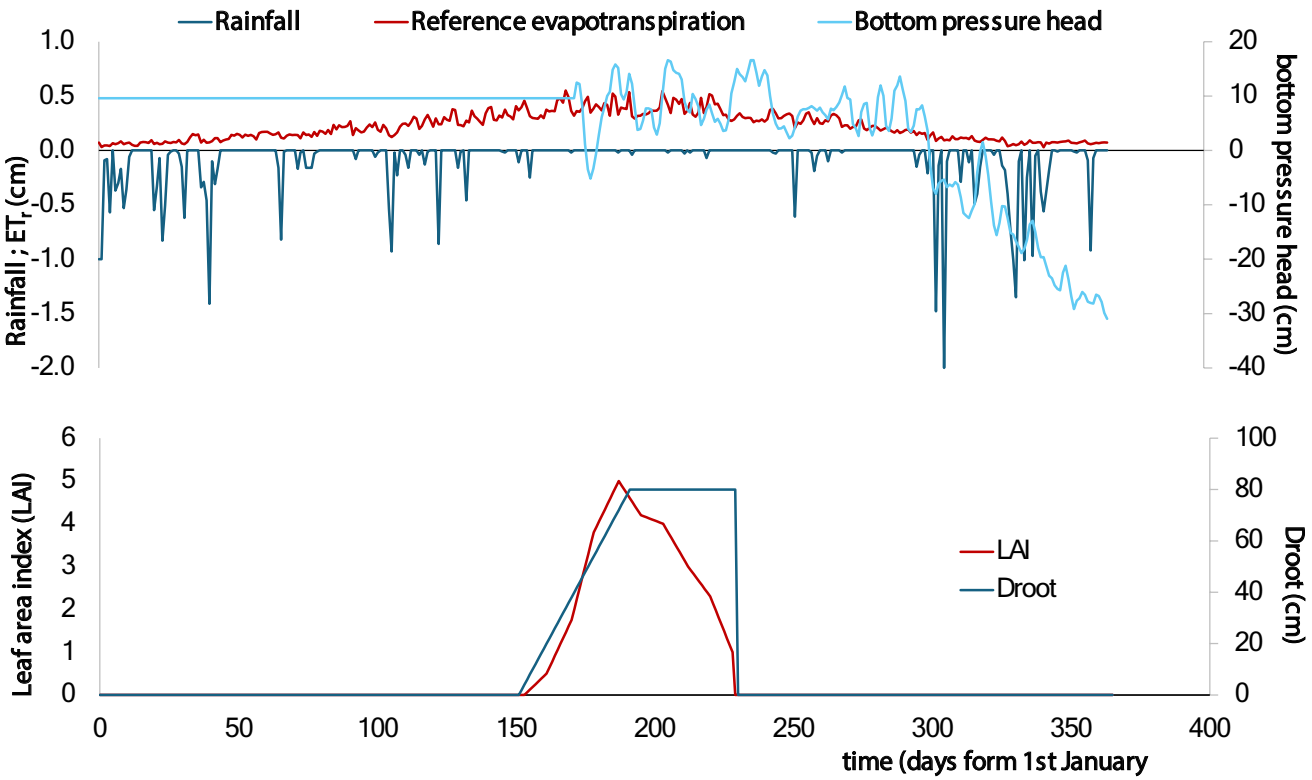


Fig. 5 Graphical view of the time-variable top and bottom boundary conditions, as well as of the time-variable vegetation conditions used for the simulation

gradient) at the bottom boundary and a bare soil (no vegetation). Again, the solid lines are for FLOWS predictions whereas blue circles are for HYDRUS simulations.

It is important to note that some flux peaks are missing in the HYDRUS results, specifically on days 2, 5, 24, 41, 307, 339 and 343. This is since HYDRUS outputs were recorded at two-day intervals, as HYDRUS-1D imposes a limitation on the number of output time steps that can be saved (250), whereas FLOWS outputs were generated at daily scale (365 printed times for one year simulation). The overall Root-Mean-Square Differences, RMSD, between HYDRUS-estimated and FLOWS-estimated fluxes was 0.14 cm/d. The overall RMSD values, between HYDRUS and FLOWS estimates, for soil water pressure heads and solute concentrations were 147.6 cm and 0.0008 g/cm^3, respectively. Additionally, some of the (minor) discrepancies between the two simulations may be attributed to differences in how the two models construct the simulation flow fields, so that the node depths may not correspond exactly between FLOWS and HYDRUS. Some differences in evapotranspiration fluxes may be due to slight variations in how the two models handle surface evaporation and root water uptake across different nodes. Nevertheless, the maximum absolute difference between the HYDRUS-estimated and the FLOWS-estimated ET was 0.93 cm/d with the overall RMSD of 0.11 cm/d.

In any case, in general, it is important to recognize that simulations derived from the numerical solution of differential equations are inherently sensitive to the numerical strategies employed. Each model adopts its own discretization schemes and solution algorithms which, while conceptually aligned, often differ in implementation details. As a result, exact agreement between different models should not be expected.

7 Conclusions

This paper provided a systematic description of the agrohydrological model FLOWS. A distinctive feature of FLOWS is its client–server architecture, which allows users to interact directly with the model through a web browser (https://flows.unica.it), eliminating the need for local installations or configurations. The entire computational load is handled by the server, which runs the main routines developed in MATLAB, while the client-side interface provides a streamlined and intuitive environment for configuring and executing simulations. The interface is designed to guide the user through the setup process with contextual suggestions and warning messages, significantly reducing the likelihood of configuration errors. This architecture makes the model accessible even to users with limited experience

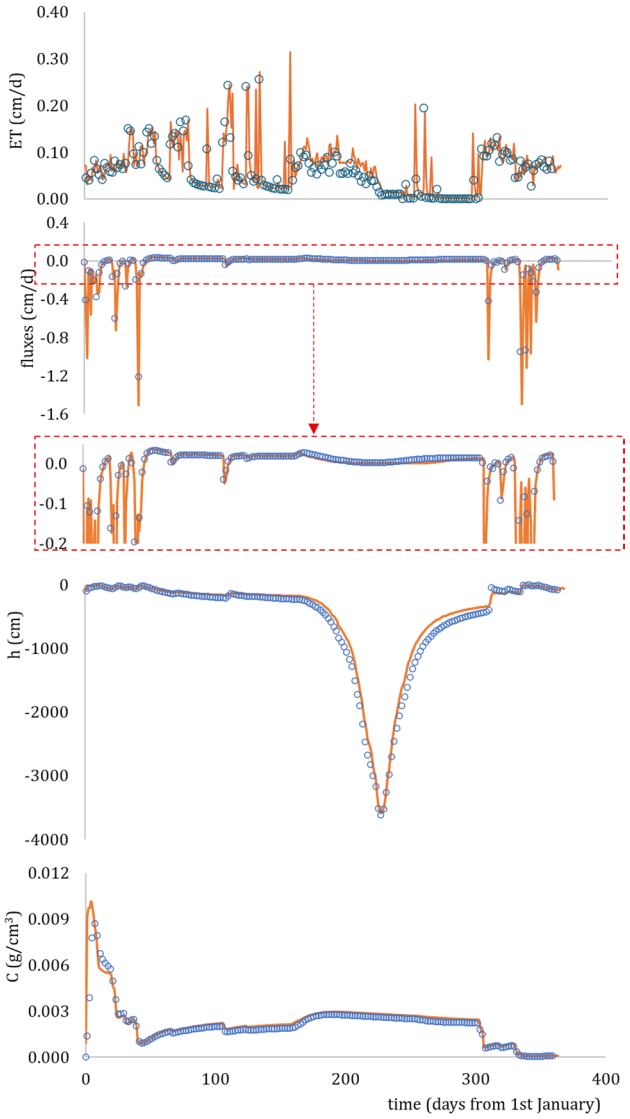


Fig. 6 Evapotranspiration fluxes and water fluxes, pressure heads, and solute concentrations at a depth of 20 cm, as predicted by the FLOWS model (solid orange lines) and the HYDRUS model (blue hollow circles). The third graph from the top is the fluxes of the second graph but only within the range between −0.2 and 0 cm/d

in physically based hydrological modeling. Nevertheless, a minimum knowledge of soil physics and calibrated parameters are required to effectively and efficiently use FLOWS.

In the paper, FLOWS was also evaluated by benchmarking its performance and numerical reliability against HYDRUS-1D. The comparison showed that FLOWS produces results highly consistent with HYDRUS-1D across diverse and complex situations, including multi-layered soils. This agreement was achieved by ensuring that all initial conditions, hydraulic parameters, boundary conditions, evapotranspiration calculations, and the Feddes stress function were identical in both models. This close match

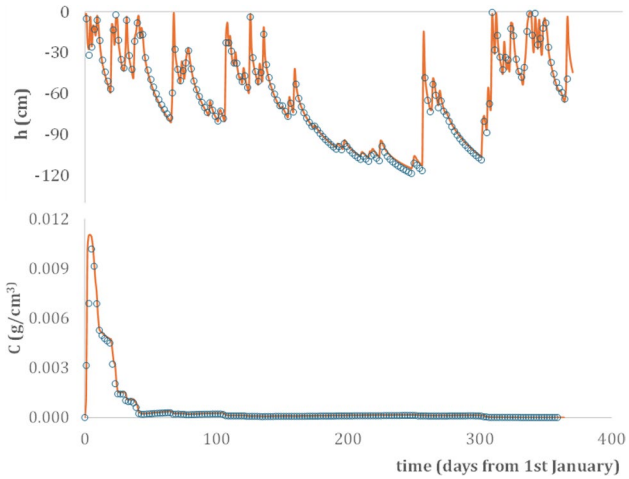


Fig. 7 Pressure heads and solute concentrations at a depth of 10 cm, as predicted by the FLOWS model (solid orange lines) and the HYDRUS model (blue hollow circles)

confirms that FLOWS possesses a level of numerical stability and robustness equivalent to well-regarded existing simulation software.

FLOWS proved to be computationally efficient, capable of completing typical one-year simulations in under a minute on standard personal computers. While factors like hardware and process complexity play a role, the speed of the numerical solution of the Richards equation was identified as the most critical determinant of total computation time.

Beyond its core performance, FLOWS offers several significant advantages for agro-hydrological research and management, among which:

1. Integrated carbon, nitrogen and phosphorus transformations and transport: It simultaneously simulates the cycles of organic carbon, nitrogen, and phosphorus along with water flow and solute movement, facilitating complete, process-based analysis.
2. Irrigation Management Tool: It supports optimizing irrigation practices (timing and volume) based on water pressure head in the root zone.
3. Multi-Site Simulation: It has the crucial ability to run simulations for multiple locations, necessary for regional or spatially distributed assessments.

The performance of FLOWS in simulating processes described at items 1 and 2 will be evaluated in a second companion paper entitled FLOWS: *A model to simulate water and solutes fluxes in agricultural and environmental systems. 2. Modules for specific applications in agro-hydrological modelling*), where Modules for specific applications in agro-hydrological modelling will be specifically shown.

Appendix: Non-linear solution procedure and time-step control algorithms

Time stepping and convergence criteria

FLOWS solves the one-dimensional Richards equation using an implicit finite-difference formulation. The nonlinearity arises from the dependence of volumetric water content, θ(h), and hydraulic conductivity, K(h), on pressure head. Particular attention is required in evaluating the differential water capacity, C = dθ/dh, because an inconsistent approximation of this storage term can directly produce water-balance errors. Nonlinear changes in hydraulic conductivity primarily affect the calculated redistribution of water within the profile [56].

The water capacity at node i and time level j + 1 is evaluated with the standard chord-slope approximation [12, 57, 58]:

$$C_i^{j+1^m} = \frac{\theta(h_i^{j+1^m}) - \theta(h_i{}^j)}{h_i^{j+1^m} - h_i{}^j} \tag{45}$$

In Eq. 45, i is the spatial node, j is the accepted time level, and m is the nonlinear iteration level. Because the water capacity depends on the unknown pressure head, the linearized tridiagonal system is solved repeatedly. After each solution, the chord-slope capacity is updated using the latest pressure-head estimate.

Following correction of the convergence check, a time step is accepted when

$$\max_{1\le i\le N} \left| h_i^{j+1^{m+1}} - h_i^{j+1^m} \right| \le \varepsilon_h \tag{46}$$

FLOWS uses a value of $\varepsilon_h = 0.001$ cm.

The iteration number M required for convergence is also used for setting an automatic variable simulation time step according to the following criteria:

$$\begin{aligned} &1.\quad \Delta t^{j+1} = 1.3\Delta t^j \quad \text{if} \quad M \le 3 \\ &2.\quad \Delta t^{j+1} = \Delta t^j \quad \text{if} \quad 3 > M < M_{max} \\ &3.\quad \Delta t^j = \frac{\Delta t^j}{3} \quad \text{if} \quad M \ge M_{max} \end{aligned} \tag{47}$$

having set the maximum iteration number $M_{max} = 10$. Note that if the convergence is not reached within 10 iterations, the attempted time step is rejected and repeated from the previous simulation time. FLOWS allows the user to specify an initial time step, Δt_{in}, as well as minimum, Δt_{min}, and maximum, Δt_{max}, allowable time steps that cannot be exceeded during the time-step adjustment procedure.

These criteria allow for a practical stability control for the nonlinear flow solution, as time steps increase during periods of smooth hydraulic response and decrease during rapid changes in boundary conditions or soil–water status.

The time step is also shortened when necessary to reach exactly a prescribed boundary-condition transition or output time.

Water balance in the soil profile

FLOWS evaluates water balance by calculating the following soil-profile cumulative residual at the last time step J:

$$R_w^J = W^J - W^0 + \sum_{j=0}^{J-1} [q_{top}{}^{j+1/2} - q_{bot}{}^{j+1/2} + \sum_{i=1}^{N} (S_{root,i}{}^{j+1/2} + S_{drain,i}{}^{j+1/2}) \Delta z_i] \Delta t_j \tag{48}$$

where W^0 and W^0 are the initial and time j soil water storages, respectively; q_{top} and q_{bot} are the top and bottom boundary fluxes, respectively' and S_{root} and S_{drain} are the sink terms for root water uptake and subsurface artificial drainage, respectively.

where the soil profile water storage, W^j is:

$$W^j = \sum_{i=1}^{N} \theta_i{}^j \Delta z_{i,CV} \tag{49}$$

A conservative calculation gives $R_w^J = 0$ apart from round-off, temporal integration, spatial discretization, and nonlinear iteration errors. Root uptake and lateral drainage represent sinks for the Richards equation.

In Eq. 48, q_{top} is the flux that actually crosses the soil surface and, thus, runoff has already been excluded before water enters the soil profile.

When ponding is active, the total storage in Eq. 48 is the sum of soil water and surface water:

$$W_{tot}{}^j = W_{soil}{}^j + W_{pond}{}^j \tag{50}$$

A Celia-type ratio is also calculated for mass balance comparison with earlier studies:

$$\mathrm{MB}_w^J = \frac{W_{tot}{}^J - W_{tot}{}^0 + L_w{}^J}{I_w{}^J} \tag{51}$$

where $I_w{}^J$ is the cumulative external water input and $L_w{}^J$ represents all cumulative water losses. Perfect conservation corresponds to $\mathrm{MB}_w^J = 1$.

Water balance of the whole simulated system

FLOWS calculates the water balance of the whole simulated system by partitioning external supply among storage, evaporation, runoff, bottom exchange, root uptake and lateral drainage. In case of a pond, infiltration from the pond into the soil is an internal transfer, as it simply decreases pond storage and increases soils water storage by the same amount and thus it does not appear in the system balance:

For the complete system, external supply is partitioned among storage, evaporation, runoff, bottom exchange, root uptake, and lateral drainage. Infiltration from the pond into the soil is an internal transfer: it decreases pond storage and increases soil storage by the same amount and therefore does not appear in the combined balance:

By considering all the quantities positive and cumulative over the last time step J, the residual for the for the combined surface–pond–soil system is:

$$R_{w,syst}^{J} = W_{soil}{}^{J} + W_{pond}{}^{J} - W_{soil}{}^{0} - W_{pond}{}^{0} - I_{ext}{}^{J} + E_{soil}{}^{J} + E_{pond}{}^{J} + R_{off}{}^{J} + Q_{bot,out}{}^{J} - Q_{bot,in}{}^{J} + U_{root}{}^{J} + D_{lat}{}^{J} \quad (52)$$

where the cumulative external water supplied to the system through rainfall, irrigation, or other specified inputs is denoted by $I_{ext}{}^{J}$. The terms $E_{soil}{}^{J}$ and $E_{pond}{}^{J}$ represent cumulative evaporation directly from the soil surface and from the free-water surface of the pond, respectively. At the lower boundary, $Q_{bot,out}{}^{J}$ represents the cumulative downward water export, whereas $Q_{bot,in}{}^{J}$ represents the cumulative upward water input. The cumulative water lost through surface runoff is denoted by $R_{off}{}^{J}$ and is calculated as:

$$R_{off}{}^{J} = \sum_{j=0}^{J-1} R_{off}{}^{j+1/2} \Delta t^{j} \quad (53)$$

Finally, $U_{root}{}^{J}$ and $D_{lat}{}^{J}$ represent the cumulative root uptake and lateral drainage fluxes over the simulation.

All these quantities are expressed as an equivalent water depth and therefore have dimensions of length, typically cm in FLOWS.

Solute mass balance in the soil profile

Similarly, for each simulated solute, FLOWS calculates the cumulative residual at the last time step J as:

$$R_{s}^{J} = M_{s}{}^{J} - M_{s}{}^{0} - M_{s,in}{}^{J} + M_{s,out}{}^{J} + M_{s,runoff}{}^{J} + M_{s,drain}{}^{J} + M_{s,uptake}{}^{J} + M_{s,loss}{}^{J} \quad (54)$$

In Eq. 54, $M_{s}{}^{J}$ is the total stored mass of the solute s per unit horizontal area (M L^{-2}) and is calculated as:

$$M_{s}{}^{j} = M_{s,diss}{}^{j} + M_{s,ads}{}^{j} + M_{s,gas}{}^{j} + M_{s,pond}{}^{j} + M_{s,reactive}{}^{j} \quad (55)$$

The dissolved mass is

$$M_{s,diss}{}^{j} = \sum_{i=1}^{N} \theta_{i}{}^{j} C_{s,i}{}^{j} \Delta z_{i} \quad (56)$$

with $C_{s,i}{}^{j}$ the dissolved concentration of the solute s at node i.

$M_{s,in}{}^{J}$ is the cumulative solute mass input; $M_{s,out}{}^{J}$ is the cumulative advective plus dispersive–diffusive boundary mass flowing from the profile. $M_{s,runoff}{}^{J}$, $M_{s,drain}{}^{J}$ and $M_{s,uptake}{}^{J}$ are the cumulative solute masses flowing to the surface runoff, to the lateral drainage and extracted by the roots, respectively. Finally, $M_{s,loss}{}^{J}$ are cumulative irreversible reaction losses, such as denitrification in case of nitrogen transport, for example.

The other terms in Eq. 55, $M_{s,ads}{}^{j}, M_{s,gas}{}^{j}, M_{s,pond}{}^{j}, M_{s,reactive}{}^{j}$ are, respectively, adsorbed solute, gas-phase solute mass, solute mass stored in the surface pond and mass in all reactive, precipitated, chemisorbed, organic, or microbial pools. All the masses in the equations above are per unit horizontal area (M L^{-2}).

According to the specific solute transport configuration, a solute specific balance is calculated. In the case of a single solute transport, FLOWS calculates the balance of the solute, including dissolved, adsorbed, and gaseous storage when active. In the case of nitrogen transport, FLOWS calculates separate NH_4^+ and NO_3^- balances and the combined mineral-nitrogen balance. Nitrification is an internal transfer; it appears with opposite signs in the two species balances and cancels in the combined balance. In case of Nitrogen and Phosphorus transport, the phosphorus balance is also calculated and includes dissolved, adsorbed, precipitated, chemisorbed, and organic phosphorus pools whenever they are simulated.

Acknowledgements This work was supported by the project "NPP-SOL—Modelling and Technological Tools to Prevent Surface and Ground-Water Bodies from Agricultural Non-Point Source Pollution Under Mediterranean Conditions", funded by the European Union—Partnership for Research and Innovation in the Mediterranean Area (PRIMA Sec.2)—CUP C83C23000100005.

Author contribution A.C. (Coppola) developed the MATLAB code, wrote the main manuscript and performed the main analyses. C.F. and A.C. (Concas) developed the Desktop graphical interface. F.P. developed the web-based code and graphical interface. A.B., A.C. (Comegna), S.B.M.H. tested the code and performed the benchmarking. S.B.M.H. participated at manuscript preparation.

Funding Open access funding provided by Università degli Studi della Basilicata within the CRUI-CARE Agreement.

Data availability No datasets were generated or analysed during the current study.

Declarations

Competing interests The authors declare no competing interests.

Open Access This article is licensed under a Creative Commons Attribution 4.0 International License, which permits use, sharing, adaptation, distribution and reproduction in any medium or format, as long as you give appropriate credit to the original author(s) and the source, provide a link to the Creative Commons licence, and indicate if changes were made. The images or other third party material in this article are included in the article's Creative Commons licence, unless indicated otherwise in a credit line to the material. If material is not included in the article's Creative Commons licence and your intended use is not permitted by statutory regulation or exceeds the permitted use, you will need to obtain permission directly from the copyright holder. To view a copy of this licence, visit http://creativecommons.org/licenses/by/4.0/.

References

1. Jensen M (1980) Design and operation of farm irrigation systems. American Society of Agricultural Engineers: St. American Society of Agricultural Engineers, St. Joseph
2. Bear J (1979) Hydraulics of groundwater. McGraw-Hill Book Inc, Mineola
3. Wagenet RJ, Hutson J (1989) LEACHM: leaching estimation and chemistry model—a process based model of water and solute movement, transformations, plant uptake and chemical reactions in the unsaturated zone. Continuum (N. Y). 2
4. van Dam JC, Huygen J, Wesseling JG et al (1997) Theory of SWAP version 2.0. In: Simulation of water flow, solute transport and plant growth in the soil–water–atmosphere–plant environment. DLO Winand Staring Centre
5. Hanson JD, Ahuja LR, Shaffer MD et al (1998) RZWQM: simulating the effects of management on water quality and crop production. Agric Syst 57:161–195. https://doi.org/10.1016/S0308-521X(98)00002-X
6. Simunek J, Van Genuchten MT, Sejna M (2005) The HYDRUS-1D software package for simulating the one-dimensional movement of water, heat, and multiple solutes in variably-saturated media. Univ Calif-Riverside Res Rep 3:1–240
7. Hansen S, Abrahansen P, Petersen CT, Styczen M (2012) Daisy: model use, calibration and validation. Trans ASABE 55:1315–1333
8. Williams JR, Renard KG, Dyke PT (1983) EPIC: a new method for assessing erosion's effect on soil productivity. J Soil Water Conserv 38:381 LP–383
9. McCown RL, Hammer GL, Hargreaves JNG et al (1996) APSIM: a novel software system for model development, model testing and simulation in agricultural systems research. Agric Syst 50:255–271. https://doi.org/10.1016/0308-521X(94)00055-V
10. Jones JW, Hoogenboom G, Porter CH et al (2003) The DSSAT cropping system model. Eur J Agron 18:235–265. https://doi.org/10.1016/S1161-0301(02)00107-7
11. Coppola A, Hassan S, Pili F (2025) FLOWS—FLOw of Water and Solutes in agricultural and environmental systems. 111
12. Coppola A, Gerke HH, Comegna A et al (2012) Dual-permeability model for flow in shrinking soil with dominant horizontal deformation. Water Resour Res. https://doi.org/10.1029/2011WR011376
13. Coppola A, Dragonetti G, Sengouga A, et al (2019) Identifying optimal irrigation water needs at district scale by using a physically based agro-hydrological model. Water (Basel). 11
14. Coppola A, Comegna A, Dragonetti G et al (2015) Simulated preferential water flow and solute transport in shrinking soils. Vadose Zone J 14:vzj2015.02.0021. https://doi.org/10.2136/vzj2015.02.0021
15. Coppola A, Zucaro R, Baralla S et al (2024) Monitoring and modelling fluxes of water and nutrients to surface drainage network from irrigated agricultural fields in a hydraulically reclaimed coastal area. Ecohydrology 17:e2723. https://doi.org/10.1002/eco.2723
16. Porru MC, Hassan SBM, Abdelmaqsoud MSM et al (2024) Using index and physically-based models to evaluate the intrinsic groundwater vulnerability to non-point source pollutants in an agricultural area in Sardinia (Italy). Front Water. https://doi.org/10.3389/frwa.2024.1399170
17. Fusco F, Allocca V, Bancheri M et al (2024) A multi-method approach for assessing groundwater vulnerability of shallow aquifers in the Marchfeld region (Austria). J Hydrol Reg Stud 54:101865. https://doi.org/10.1016/j.ejrh.2024.101865
18. Hassan SBM, Dragonetti G, Comegna A et al (2024) Analyzing the role of soil and vegetation spatial variability in modelling hydrological processes for irrigation optimization at large scale. Irrig Sci. https://doi.org/10.1007/s00271-023-00882-7
19. Kroes JG, Van Dam JC, Groenendijk P et al (2008) SWAP version 3.2. theory description and user manual
20. van Dam JC, Groenendijk P, Hendriks RFA, Kroes JG (2008) Advances of modeling water flow in variably saturated soils with SWAP. Vadose Zone J 7:640–653. https://doi.org/10.2136/vzj2007.0060
21. Kuznetsov M, Yakirevich A, Pachepsky YA et al (2012) Quasi 3D modeling of water flow in vadose zone and groundwater. J Hydrol (Amst) 450–451:140–149. https://doi.org/10.1016/j.jhydrol.2012.05.025
22. van Genuchten MTh (1980) A closed-form equation for predicting the hydraulic conductivity of unsaturated soils. Soil Sci Soc Am J 44:892–898. https://doi.org/10.2136/sssaj1980.03615995004400050002x
23. Russo D (1988) Determining soil hydraulic properties by parameter estimation: on the selection of a model for the hydraulic properties. Water Resour Res 24:453–459. https://doi.org/10.1029/WR024i003p00453
24. Coppola A (2000) Unimodal and bimodal descriptions of hydraulic properties for aggregated soils. Soil Sci Soc Am J 64:1252–1262. https://doi.org/10.2136/sssaj2000.6441252x
25. Durner W (1994) Hydraulic conductivity estimation for soils with heterogeneous pore structure. Water Resour Res 30:211–223. https://doi.org/10.1029/93WR02676
26. Ross PJ, Smettem KRJ (1993) Describing soil hydraulic properties with sums of simple functions. Soil Sci Soc Am J 57:26–29. https://doi.org/10.2136/sssaj1993.03615995005700010006x
27. Mualem Y (1976) A new model for predicting the hydraulic conductivity of unsaturated porous media. Water Resour Res 12(3):513–522. https://doi.org/10.1029/WR012i003p00513
28. Gardner WR (1958) Some steady-state solutions of the unsaturated moisture flow equation with application to evaporation from a water table. Soil Sci 85:228–232
29. Feddes RA, Raats PAC (2004) Parameterizing the soil–water–plant root system. In: Drugs of the future. pp 844–845
30. Feddes RA (1978) Simulation of field water use and crop yield. Centre for Agricultural Publishing and Documentation (PUDOC), Wageningen. https://edepot.wur.nl/168026
31. Raats PAC (1974) Steady flows of water and salt in uniform soil profiles with plant roots. Soil Sci Soc Am J 38:717–722. https://doi.org/10.2136/sssaj1974.03615995003800050012x

32. Prasad R (1988) A linear root water uptake model. J Hydrol (Amst) 99:297–306. https://doi.org/10.1016/0022-1694(88)90055-8
33. Vrugt JA, Hopmans JW, Šimunek J (2001) Calibration of a two-dimensional root water uptake model. Soil Sci Soc Am J 65:1027–1037. https://doi.org/10.2136/sssaj2001.6541027x
34. Jarvis NJ (1989) A simple empirical model of root water uptake. J Hydrol (Amst) 107:57–72. https://doi.org/10.1016/0022-1694(89)90050-4
35. Shouse PJ, Ayars JE, Šimůnek J (2011) Simulating root water uptake from a shallow saline groundwater resource. Agric Water Manag 98:784–790. https://doi.org/10.1016/j.agwat.2010.08.016
36. Van Genuchten MT (1987) A numerical model for water and solute movement in and below the root zone. United States Department of Agriculture Agricultural Research Service US
37. Maas EV, Hoffman GH (1977) Crop salt tolerance—current assessment. J Irrig Drain Div 103:115–134. https://doi.org/10.1061/JRCEA4.0001137
38. van Genuchten MT, Hoffman GH (1984) Analysis of crop salt tolerance data. In: Soil salinity under irrigation: processes and management, pp 258–271
39. Skaggs TH, Shouse PJ, Poss JA (2006) Irrigating forage crops with saline waters: 2. Modeling root uptake and drainage. Vadose Zone J 5:824–837. https://doi.org/10.2136/vzj2005.0120
40. Maas EV, Grattan SR (1999) Crop yields as affected by salinity. In: Agricultural drainage. pp 55–108
41. Maas EV (1990) Crop salt tolerance. In: Agricultural salinity assessment and management manual, pp 262–304
42. Maas EV (1986) Salt tolerance of plants. Appl Agric Res 1:12–25
43. US Salinity Lanboratory Staff (1954) Diagnosis and improvement of saline and alkali soils. In: USDA Handbook. United States Department of Agriculture, pp 83–100
44. Skaggs TH, van Genuchten MT, Shouse PJ, Poss JA (2006) Macroscopic approaches to root water uptake as a function of water and salinity stress. Agric Water Manag 86:140–149. https://doi.org/10.1016/j.agwat.2006.06.005
45. Wadleigh CH (1946) The integrated soil moisture stress upon a root system in a large container of saline soil. Soil Sci 61:219–238
46. Meiri A, Shalhevet J (1973) Crop growth under saline conditions BT. In: Yaron B, Danfors E, Vaadia Y (eds) Arid zone irrigation. Springer, Berlin, pp 277–290
47. Childs SW, Hanks RJ (1975) Model of soil salinity effects on crop growth. Soil Sci Soc Am J 39:617–622. https://doi.org/10.2136/sssaj1975.03615995003900040016x
48. du Plessis HM (1985) Evapotranspiration of citrus as affected by soil water deficit and soil salinity. Irrig Sci 6:51–61. https://doi.org/10.1007/BF00272475
49. Bresler E, Hoffman GJ (1986) Irrigation management for soil salinity control: theories and tests. Soil Sci Soc Am J 50:1552–1560. https://doi.org/10.2136/sssaj1986.03615995005000060034x
50. Shalhevet J, Hsiao ThC (1986) Salinity and drought. Irrig Sci 7:249–264. https://doi.org/10.1007/BF00270435
51. Mollerup M, Abrahamsen P, Petersen CT, Hansen S (2014) Comparison of simulated water, nitrate, and bromide transport using a Hooghoudt-based and a dynamic drainage model. Water Resour Res 50:1080–1094. https://doi.org/10.1002/2012WR013318
52. Hooghoudt SB (1940) General consideration of the problem of field drainage by parallel drains, ditches, watercourses, and channels. In: Contribution to the knowledge of some physical parameters of the soil, vol 7
53. Selim HM, Amacher MC (1996) Reactivity and transport of heavy metals in soils. CRC Press, Boca Raton
54. Wallach R, van Genuchten MT (1990) A physically based model for predicting solute transfer from soil solution to rainfall-induced runoff water. Water Resour Res 26:2119–2126. https://doi.org/10.1029/WR026i009p02119
55. Van Wijk WR, De Vries DA (1963) Periodic temperature variations in a homogeneous soil. Phys Plant Environ 1:103–143
56. Jensen KH (1983) Simulation of water flow in the unsaturated zone including the root zone. Series Paper No. 33, Institute of Hydrodynamics and Hydraulic Engineering, Technical University of Denmark, Lyngby, 259 pp. https://agris.fao.org/search/en/providers/122514/records/64774d96a3fd11e430387c06
57. Huang K, Mohanty BP, Van Genuchten MT (1996) A new convergence criterion for the modified Picard iteration method to solve the variably saturated flow equation. J Hydrol (Amst) 178:69–91. https://doi.org/10.1016/0022-1694(95)02799-8
58. Rathfelder K, Abriola LM (1994) Mass conservative numerical solutions of the head-based Richards equation. Water Resour Res 30:2579–2586. https://doi.org/10.1029/94WR01302

Publisher's Note Springer Nature remains neutral with regard to jurisdictional claims in published maps and institutional affiliations.